Agronomy Research **11** (1), 73–80, 2013

The mathematical model of segmented capacitance sensor with grounded segments for determining of material distribution on the conveyor

J. Lev[1,*], V. Prošek[2], M. Wohlmuthová[3] and F. Kumhála[1]

[1]Department of Agricultural Machines, Faculty of Engineering, Czech University of Life Sciences Prague, Kamýcká 129, 16521 Prague 6, Czech Republic; [*]Correspondence: jlev@tf.czu.cz
[2]Department of Machinery Utilisation, Faculty of Engineering, Czech University of Life Sciences Prague, Kamýcká 129, 16521 Prague 6, Czech Republic
[3]Department of Mathematics, Faculty of Engineering, Czech University of Life Sciences Prague, Kamýcká 129, 16521 Prague 6, Czech Republic

Abstract. The need to analyse the material flow on conveyors is an important issue not only in agriculture but also in a number of industries. One of the possibilities is the use of electrical capacitive sensors. In the past, simple throughput capacitive sensors, but also very sophisticated electrical capacitance tomographs were tested. A compromise may be a segmented capacitance sensor. Functional principle is based on the capacitive measurement of the mixture of material and air several times. From the measured data it is then possible to determinate the parameters of the material distribution. This process is commonly called image reconstruction. The reconstruction algorithm is very important for development of the mathematical model of the sensor. In this paper the proposed mathematical model for the sensor with grounded SCS segments was evaluated. This variant of a possible sensor configuration is relatively simple, however, the sensitivity of the sensor in response to changes in the distribution of material within the sensing area is reduced. To verify the mathematical model, a laboratory experiment was designed. Tested sample was moved inside the sensing area and the response of the sensor was observed. Proposed mathematical model was confirmed by this measurement. On the base of measurement results, proposed mathematical model can be used in the development of reconstruction algorithm.

Key words: segmented capacitance sensor, mathematical model, material distribution, throughput.

INTRODUCTION

Yield maps are an important source for the practical application of precision agriculture. Creating of yield maps requires a high-quality system for measurement of the actual throughput, preferably during the harvest. Capacitive sensor technique might be a good alternative for instantaneous throughput measurement. The advantages of a capacitive sensor are its non-contact way of measurement, its relative simplicity, its possible suitability for the often difficult operating conditions found on agricultural

machines (e.g., Stafford et al., 1996, reported that the sensor based on electrical capacitance can be constructed to meet the criteria of minimal impedance to the flow material and of insensitivity to mechanical vibrations), its low cost and its easy installation on the machinery (Savoie et al., 2002).

Capacitive sensor techniques can be used to determine different properties of a range of plant materials. The function of capacitive sensors depends on the fact that the dielectric constant of an air/material mixture between two parallel plates increases with the material volume concentration increasing. Capacitive sensors have been widely used for plant material moisture content determination (Eubanks & Birrell, 2001; Lawrence et al., 2001; Osman et al., 2002; Snell et al., 2002).

In the Department of Agricultural Machines, Faculty of Engineering of CULS Prague the capacitive throughput sensor for plant material throughput measurement has been developed in recent years. It can be used for measurement of the actual plant or other materials throughput. This sensor for forage, potatoes, sugar beet, chopped maize and hop throughput measurement was tested (Kumhála et al., 2009; Kumhála et al., 2010). In virtually all these cases positive functioning was confirmed. Only, during forage throughput measurements were the results worse. However, the forage is very complicated material.

This sensor, like most other methods used for measurement of actual data (Martel & Savoie, 1999; Hennens et al., 2003; Reinke et al., 2011), has only one output signal from which only the amount of material can be inferred while its distribution cannot. This fact was the inspiration for the beginning of development of the segmented capacitance sensor (SCS) (Kumhála et al., 2012).

The principle of SCS function is based on multiple measurements of the air and material mixture electrical capacity. Material properties can be determined from measured data. The principle function of SCS is similar to the principle of electrical capacitance tomography (ECT). About the ECT wrote such Yang (2010), or also Xie et al. (1992). The example of ECT sensor functioning can be as follows. The ECT sensor with 12 electrodes is considered. In the first step, to obtain a complete set of data for one image, electrode 1 is used for excitation and electrodes 2–12 for detection, obtaining 11 capacitance measurements. In the next step, electrode 2 is used for excitation and electrodes 3–12 for detection, obtaining 10 capacitance measurements. This process continues until electrode 11 is used for excitation and electrode 12 for detection, obtaining only one capacitance measurement. In this case, there will be 66 independent capacitance measurements. In general, the number of independent capacitance measurements is governed by $N\,(N-1)/2$, where N is the number of electrodes. Measured changes in capacity between excitation and detection electrodes are very small and also measuring ranges vary according to the order of electrodes between which it is measured. The demands on measuring device quality are relatively high for that reason.

It is obvious that the ECT has long been dealt with. ECT sensors are relatively complicated and expensive. SCS may be less complicated, cheaper and quality imaging could be comparable. In a recent article (Lev et al., 2013), we have dealt with the proposal of SCS, where were expected ‘released segments’ and ‘floating potentials’.

Multiple measurements were proposed as follows. The sensor was composed of two plates. The bottom plate was grounded and undivided. The upper plate was divided into eight segments. It was considered eight measurements. During one measurement

one segment was connected to the measuring circuit and measured electrical capacitance between it and the other grounded elements. Segments that were not exactly used to measure were isolated from the ground and, of course, from the measuring circuit. These segments were labelled as 'released segments'. Although released segments were not used directly to measure, its effect was significant. Due to floating potentials in the areas of segments there is a significant shaping of the electric field sensor. As for the image reconstruction it is desirable to have a reliable mathematical model of an electric field, it is necessary to calculate the values of floating potential with sufficient accuracy. This can be problematic, because the values of floating potentials can be affected by parasitic capacitances in real conditions. These parasitic capacitances are typically made up of a switch that connects and disconnects the segment to the measurement circuit.

One of the ways to work around this problem is to connect the segments that are not exactly used to measure with zero potential. In the mathematical model the domains of segments will be removed and on their edges Dirichlet boundary conditions will be defined. This step simplifies the mathematical model, but certainly also reduces the sensitivity of the sensor. In this paper, the mathematical model with grounded SCS segments is evaluated.

MATERIALS AND METHODS

The scheme of experimental model of the segmented capacitance sensor (SCS) can be seen on Fig. 1. Design of SCS is very simple. The basic parts of SCS are upper measuring segments and bottom measuring plate. All electrodes are made from cuprexit 1.5 mm thick. Cuprexit is an insulating material, which is coated by a copper layer of 35 μm thickness. Measuring segments are 504 mm wide and 252 mm long. The width of the bottom plate is 504 mm and its length is the same as for the measuring segments, i.e. 252 mm. Another important part of SCS is the frame on which the above described electrodes are placed. The frame consists of kartit plates 12 mm thick. Kartit is an electro-insulating material. And the last but not least important part (Fig. 1) is the earthed steel cage, which is used for shielding in order to remove the influence of surrounding effects. The sensing area bounded by electrodes and the dimension of the frame of the sensor are 510 mm in width and 126 mm in height. The whole area bounded by a steel case is 1,000 mm in width and 500 mm in height.

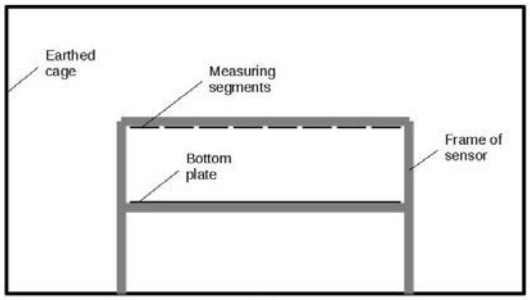

Figure 1. Experimental model scheme of segmented capacitance sensor (SCS).

The task of the mathematical model is to describe the electric field of the sensor. This field affects first of all test segments but also grounded elements of sensor and the frame, the test sample in the sensing area and all other elements of the sensor. The electric field is energised with alternating current at a frequency of 6 MHz. This frequency was chosen based on previous experience. It is a compromise between the low and high frequency. At low frequencies, the impedance of the sensor is too large and the measurement is complicated. At high frequencies, the measurement circuit becomes unstable. Nevertheless, it is a variable electric field; a number of authors (Williams & Beck, 1995; Fuchs & Zangl, 2007; Yang, 2010) use the Laplace equation for its description which describes the electrostatic field:

$$-\nabla(\varepsilon \cdot \nabla\varphi) = 0 \tag{1}$$

where $\varepsilon = \varepsilon_0.\varepsilon_r$, where ε_0 is the permittivity of vacuum, ε_r is the relative permittivity of surroundings and φ is the scalar electric potential. The validity of this model was also demonstrated by our recent experiments (Lev et al., 2013).

The situation that was simulated is as follows. The sample was moved within the sensing area. The sample was made up of the prism with a square cross section of 40 mm by 40 mm. Material of the sample was moistened balsa wood. The sample was successively placed in the sensing area on the bottom plate at seven different positions, which were evenly spaced, but not completely symmetrical relative to the centre axis of the sensor. All samples were slightly shifted to the left by 12 mm. Distances between the individual positions were 63 mm. The relative permittivity of the sample was estimated $\varepsilon_r = 100$. The exact value is not important because the value of the electric field intensity decreases rapidly with the increasing of the relative permittivity (when the surroundings have a significantly lower relative permittivity – such as air).

For the purpose of verifying the mathematical model four electrodes were connected to the measuring circuit and the remaining four electrodes were connected to the neutral. On the edges of electrodes connected to the measuring circuit Dirichlet boundary conditions $\varphi_\Gamma = 1$ V were defined. Dirichlet boundary conditions $\varphi_\Gamma = 0$ V were also defined on the edges of the elements that were connected to the grounding conductor. Schema situation is shown in Fig. 2.

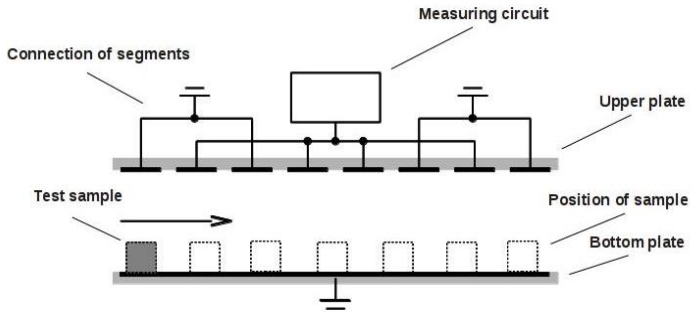

Figure 2. Scheme of the measurement process. In the sensing area there are shown seven positions of the sample. The connection of segments is plotted in the top of the image.

Equation (1) was solved by the finite element method using Agros2D software. This software is able to work with p-elements and nonconformist networks (Karban et al., 2013). It was the solution of the problem preferable for use. To calculate the capacitance changes the following equation was used:

$$C = \frac{1}{U^2} \int_V ED \, dV \tag{2}$$

where C is the electrical capacity, U is electrode-to-electrode voltage, E is the intensity of electric field, D is the electric displacement and V is the domain of the problem solved.

To measure capacity changes, the measuring circuit was used on the same basis as in Kumhála et al. (2009). The basis of this circuit it is the dividing circuit. The voltage on measuring segments and the voltage on the reference resistor is compared. Voltage change corresponds to the reactance change or electric capacity of the sensor, respectively. If the voltage change is relatively small (up to about 3%) it may be considered that the dependence of voltage changes and capacity changes is linear.

Two measurements were performed. The first measurement was carried out with a sample of the same length as the depth of the sensor. Prism length was 250 mm. The second measurement was performed with a shortened sample. Sample length was 100 mm. Both measurements were repeated 10 times.

RESULTS AND DISCUSSION

Results from the measurements and calculated values of the mathematical model are reported in Table 1. The calculated capacity changes and measured voltage changes cannot be directly compared. It is necessary to recalculate the values on the relative changes for this purpose:

$$H_r = \frac{\Delta H}{\Delta H_{100}} \times 100 \tag{3}$$

where H_r is the relative change of voltage / electric capacity, ΔH is the measured change of voltage / calculated capacity induced by placing of the sample, ΔH_{100} is the reference voltage change / calculated capacity caused by the sample in the reference position. In this case, the selected reference location was the fourth of them.

The results are divided into three sections in Table 1. In the first section the results calculated from a mathematical model can be seen. Second section shows the results of measurements with the sample 250 mm long and the third one shows the results from the measurements with the sample of 100 mm length. Both measurements are also supplemented by the values of relative errors. Measurement errors are calculated at $\alpha = 0.05$ significance level. The comparison of both measurements shows that the measurement using a longer sample was more stable. This is logical, because in this measurement the whole depth of sensor was used. Measurement errors of longer samples ranged from 0.6% to 1.9%. For measurements with a shorter sample it was

from 0.7% to 4.0%. It can also be noted that significant differences were not found between these two measurements.

Table 1. Comparison of measured and calculated values

Position of sample	1.	2.	3.	4.	5.	6.	7.
Calculated values–relative change [%]	21.5	45.1	60.3	100	77.8	47.6	34.1
Measurement–long sample [%]	20.7	45.3	59.6	100	79.6	48.4	36.4
The relative measurement error [%]	1.9	1.6	1.2	0.6	0.7	1.2	1.8
Measurement–short sample [%]	20.2	43.8	58.3	100	79.1	47.7	35.6
The relative measurement error [%]	4.0	2.7	3.4	0.7	1.9	2.7	3.3

When comparing results of the mathematical model and measurement results it can be stated that the results are almost identical. Minor differences may be caused by geometric imperfections and inaccuracy of the numerical solution. Conformity of measurement results with short and long samples also indicates that there was no significant influence of the 3D effect. This is probably due to the smaller sample sizes. The influence of the 3D effect would be probably manifested if a sample of larger dimensions was used. The 3D effect means in this case that the electric field distribution between the 2D model and the real sensor is different. The 2D model describes the electric field in the centre of the sensor. However, the electric field distribution on the edge of the sensor is different (Lev et al., 2013).

Fig. 3 shows the distribution of the electric field intensity in the sensing area of SCS. The part a) is a model describing the behaviour of 'released segments' and part b) is a model describing grounded segments. It is evident that the variant with grounded electrodes leads to a high energy concentration near to the active and grounded electrodes. It is obvious that in these locations the sensor is very sensitive to a change of permittivity distribution. However, in areas close to the bottom plate of the sensor sensitivity considerably reduces. It is possible to confirm the original premise predicting this behaviour for this reason. This is the main disadvantage of this type of arrangement of electrodes.

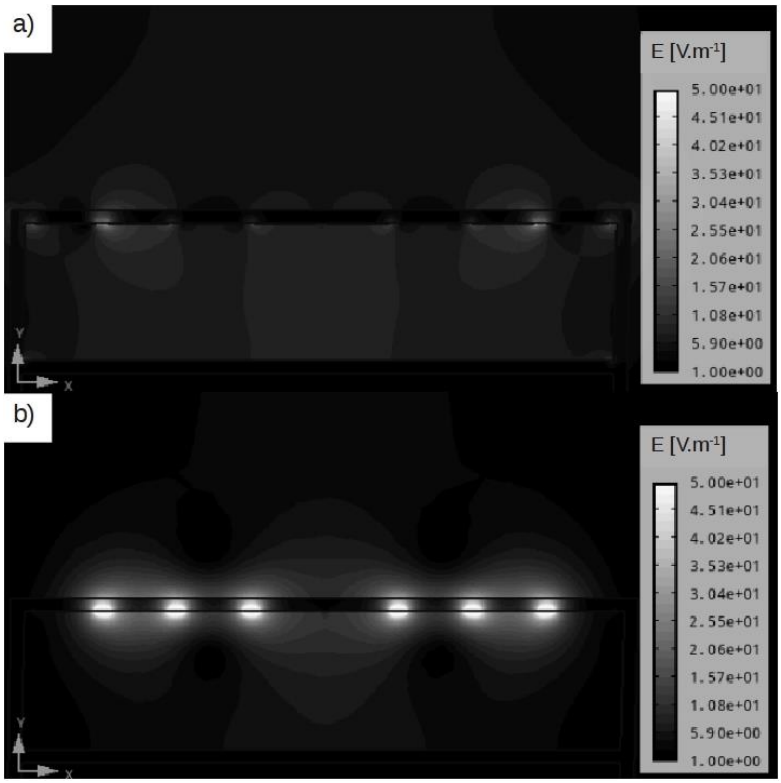

Figure 3. The distribution of the electric field in the sensing area of SCS. Connected to the measuring circuit 2, 4, 5, and 7 segment left. a) segments that are not connected to the measuring circuit are used as 'released segments', b) segments that are not connected to the measuring circuit are connected to zero potential.

CONCLUSION

The main task of this paper was to create a mathematical model of SCS and verify its validity by measurement. Measurements were performed with two types of samples (shorter sample of 100 mm and longer sample of 250 mm long). For both measurements were found the same values of relative changes in output voltage. The obtained values were compared with results from a mathematical model. Based on the comparison it can be stated that the measurements sufficiently confirmed the mathematical model and this model can be used for the development of a reconstruction algorithm.

ACKNOWLEDGEMENTS. This work was supported by the Internal Grant Agency – Faculty of Engineering, Czech University of Life Sciences Prague, Project No. 31160/1312/3111.

REFERENCES

Agros2D. [online] [10.1.2013]. Available at: http://agros2d.org.

Eubanks, J.C. & Birrell, S.J. 2001. Determining moisture content of hay and forages using multiple frequency parallel plate capacitors. *ASAE Paper* No. 011072.

Fuchs, A. & Zangl, H. 2007. Analysis of a Capacitive Mass Flow Sensor for a Screw Conveyor. **In:** *Excerpt from the Proceedings of the COMSOL Users Conference*, Grenoble.

Hennens, D., Baert, J., Broos, B., Ramon, H. & Baerdemaeker, J. De. 2003. Development of a Flow Model for the Design of a Momentum Type Beet Mass Flow Sensor. *Biosystems Engineering*. **85**(4), 425–436.

Karban, P., Mach, F., Kůs, P., Pánek, D. & Doležal, I. 2013. Numerical solution of coupled problems using code Agros2D. *Computing*. DOI 10.1007/s00607-013-0294-4. In print.

Kumhála, F., Lev, J., Wohlmutová, M. & Prošek, V. 2012. First tests with segmented capacitive throughput sensor. *Scientia agriculturae bohemica.* **43**(1) 22–27.

Kumhála, F., Prošek, V. & Blahovec, J. 2009. Capacitive throughput sensor for sugar beets and potatoes. *Biosystems Engineering.* **102**(1), 36–43.

Kumhála, F., Prošek, V. & Kroulík, M. 2010. Capacitive sensor for chopped maize throughput measurement. *Computers and Electronics in Agriculture.* **70**(1), 234–238.

Lawrence, K.C., Funk, D.B. & Windham, W.R. 2001. Dielectric moisture sensor for cereal grains and soybeans. *Transaction of ASAE*. **44**, 1691–1696.

Lev, J., Mayer, P.,·Wohlmuthová, M. & Prošek, V. 2013. The mathematical model of experimental sensor for material distribution detecting on the conveyor. *Computing.* DOI 10.1007/s00607-012-0273-1. In print.

Martel, H. & Savoie, P. 1999. Sensors to measure forage mass flow and moisture continuously. *ASAE paper* No. 991050.

Osman, A.M., Savoie, P., Grenier, D. & Theriault, R. 2002. Parallel-plate capacitance moisture sensor for hay and forage. *ASAE paper* No. 021055.

Reinke, R., Dankowicz, H., Phelan, J. & Kang, W. 2011. A dynamic grain flow model for a mass flow yield sensor on a combine. *Precision Agriculture.* **12**, 732–749.

Savoie, P., Lemire, P. & Theriault, R. 2002. Evaluation of five sensors to estimate mass-flow rate and moisture of grass in a forage harvester. *Applied Engineering in Agriculture*. **18**, 389–397.

Snell, H.G.J., Oberndorfer, C., Lücke, W. & Weghe, H.F.A. van den. 2002 Use of electromagnetic fields for the determination of the dry matter content of chopped maize. *Biosystems Engineering*. **82**, 269–277.

Stafford, J.V., Ambler, B., Lark, R.M. & Catt, J. 1996. Mapping and interpreting the yield variation in cereal crops. *Computers and Electronics in Agriculture.* **14**, 101–119.

Williams, R.A. & Beck, M.S. (eds), 1995. *Process tomography, principles, techniques and applications.* Butterworth-Heinemann, Oxford.

Xie, C.G., Huang, S.M., Hoyle, B.S., Thorn, R., Lenn, C., Snowden, D. & Beck, M.S. 1992. Electrical capacitance tomography for flow imaging-systemmodel for development of image reconstruction algorithms and design of primary sensors. **In:** *IEE Proceedings-g*, pp. 89–98.

Yang, W.Q. 2010. Design of electrical capacitance tomography sensors. *Measurement Science and Technology.* **21**, 1–13.